Optimization of via points: bridging the gap between simulation speed and biological fidelity of musculoskeletal models

Calin Vasile Simon - 4969324

***Abstract*—When designing musculoskeletal models for forward simulation studies, a tradeoff must be made between biological fidelity and computational efficiency. A method is proposed that optimizes the coordinates of via points of muscle paths, used in relatively simple musculoskeletal models, such that the muscle moment arms match those of more complex models and experimentally measured moment arms. For this purpose, the via points of the Gait2392 model are optimized to match muscle moment arms of the Rajagopal2015 model and other experimentally obtained muscle moment arms. The results show that muscles that can be represented by straight lines, can be optimized well. More complex muscles that contribute to multi-degree of freedom movements, are still improved, but to a less extent. The main benefit of the optimized model, is that the compatution time of human motion simulation is greatly improved, making it a viable option to pre-train neuromuscular controllers, which can be further fine-tuned with the more complex models. To further improve musculoskeletal models in general, more data on muscle moment arms is needed, especially for muscles that contribute to multiple joints and movements in multiple planes of motion.**

CONTENTS

I. INTRODUCTION

There is a vast interest in simulating human motion with musculoskeletal models, because it provides a non-invasive method to quantify certain metrics of human motion that can not be measured in vivo. These metrics include, but are not limited to, muscle force, muscle activation and joint contact forces. One important design choice that influences the biological fidelity of a musculoskeletal model, is the method with which the geometry of the muscle path is defined. The geometry of the muscle path determines the length of the muscle moment arm, which in turn determines the moment a muscle force exerts around a joint. Furthermore, the geometry of the muscle path also determines the velocity with which the muscle length changes as a function of joint angular velocity, which in turn influences the maximal force of the muscle through the force-velocity relationship [1].

The methods used to define muscle path geometry can be divided into two categories: the finite element models and the wired models. Finite element models are the most biologically accurate, and can represent the true geometric muscle deformations very well [2]. The wired models can be implemented in different ways:

1) Muscles can be modelled as **straight lines** from origin to insertion [3]. For some muscles this might be a good enough choice, but in some cases it is not. Take for example rectus femoris with its origins on anterior inferior iliac spine and ilium above acetabulum; and its insertion on the tibial tuberosity via patellar ligament. If the path of this muscle is modelled with a straight line, and the knee joint is rotated from extension to flexion, the muscle path will pass through anatomical structures and will end up posterior to the knee joint. This will cause rectus femoris to exert a flexion moment around the knee. For these types of situations the muscle ought to wrap around diverse anatomical structures.
2) Muscle paths can also be divided into multiple segments by adding **via points**, where the muscle force is transfered from via point to via point. An example is given in Fig. 1a, where psoas is modelled with five points to prevent the muscle from passing through anatomical structures. The upper three points are fixed in the coordinate frame of the pelvis and the fourth and fifth points are fixed in the coordinate frame of femur. Since the via points are fixed in the coordinate frames of the segments, the change in muscle length as a function of joint angle is defined solely by the displacement of the via points that span the joint. As a result, the line of action of the muscle force, and therefore also the moment arm, is also defined by the same via points. One of the major drawbacks of using via points, is that via points can cross each other during joint rotation. This problem is visualized in the right image of Fig. 1a, where the hip is rotated at 70° hip flexion, which is still well within the range of motion of the hip. The implication of this is that psoas now exerts an extension moment around the hip, which is biologically incorrect. Another major drawback of the use of via points, is that the relative change in muscle length is overestimated during axial rotations, especially if these via points are modelled closely together. A solution would be to manually tune the via points, such that these problems do not occur.

All authors are with the institute Technische Universiteit Delft c.v.simon@student.tudelft.nl

However, besides the fact that this is quite cumbersome, one has to take into account that the muscle moment arm can be highly sensitive to the position of the two via points that span the joint. Another solution would be to replace one of the via points with a conditional via point. Conditional via points are modelled such that they appear or disappear depending on the joint angle. The problem with conditional via points however, is that they disrupt the continuity of muscle parameters during joint movement, which in turn affects the biological fidelity of the musculoskeletal model and the fluidity of the simulated movement.

3) One way to resolve the issues that arise from using via points, is to add **wrapping surfaces**, which are spherical, ellipsoidal or cylindrical surfaces that are placed around the joint. Muscles are constrained to not pass through these surfaces, as seen in Fig. 1b.

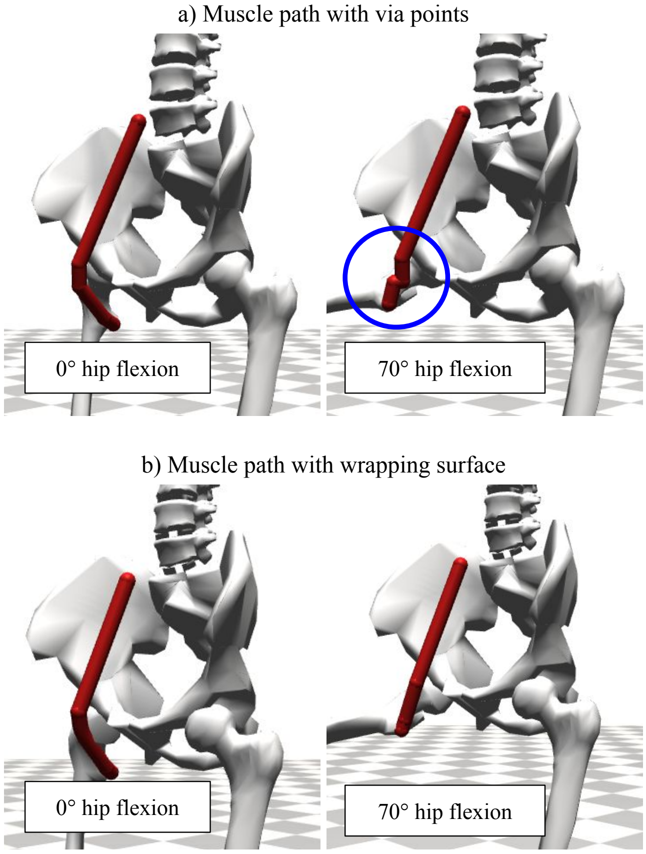

Fig. (1) a) Psoas muscle path with via points at 0° and 70° hip flexion. b) Psoas muscle path that wraps around a wrapping surface at 0° and 70° hip flexion.

Finite element muscle models and wrapping surfaces are techniques that add a lot of computational complexity to musculoskeletal models. One could argue that regardless of the computational complexity, musculoskeletal models should always represent the biological musculoskeletal system as accurately as possible. Unfortunately, this is impractical for many simulation studies. This is especially true for forward simulation studies, where the model's equations of motion are integrated forward in time to generate a motion that results from given forces. These forces are not known beforehand. Instead, a neuromuscular controller must be optimized to produce a set of forces that generate a specific movement. The optimization of the neuromuscular controller can require hundreds or thousands of iterations that all need to be simulated [4]. For these types of studies, researchers often resort to the more simple musculoskeletal models, where the muscle paths are defined with straight lines and via points, at the cost of reducing biological fidelity.

The goal of my research is to propose a method which increases the biological fidelity of lower body musculoskeletal models that are used in forward simulation studies. This is done by optimizing the position of the via points, such that the muscle moment arms assimilate the muscle moment arms of more complex models. Furthermore, the method is devised in such a way, that muscle moment arm data of the more complex models can be replaced by experimental data that is published in literature. During my literature study, I collected and organized the available moment arm data of 55 muscles around the ankle, knee and hip joint, from 31 articles, which resulted in 211 data files that describe the relations between muscle moment arms and joint angles. However, not all 2D moment arms of the 55 muscles are available. For example, bi-articular semimembranosus spans the hip joint, which can be seen as a 3 degree of freedom joint, and the knee joint, which can be seen as a 1 degree of freedom joint. In an ideal situation, we want the knee flexion, hip flexion, hip adduction and hip rotation moment arm of semimembranosus for all possible combinations of joint angles. Unfortunately, experimental data for semimembranosus is not complete and only available for the knee flexion moment arm as a function of knee flexion angle [5]–[9], and the hip flexion moment arm as a function of hip flexion angle [5]. Furthermore, there are seven different measuring methods used to determine muscle moment arm length. This is done both in vivo and in vitro, and on different types of populations, ranging from children to elderly cadavers, resulting in inconsistent measurement results. However, the users of the proposed method can choose which experimental data fits their model best and use this data as the target for the optimization. For example, researchers that want to create a model that represents elderly people, might want to use available experimental data measured on elderly cadavers for the optimization.

II. Methods

The Gait2392 model, a model which uses solely via points, is optimized to match muscle moment arm data of the Rajagopal2015 model. For most muscles, muscle moment arm data of the Rajagopal2015 falls within the range of experimental data which I collected during my literature study. For some muscles, the muscle moment arms of the Rajagopal2015 model do not match available experimental data. This was true for

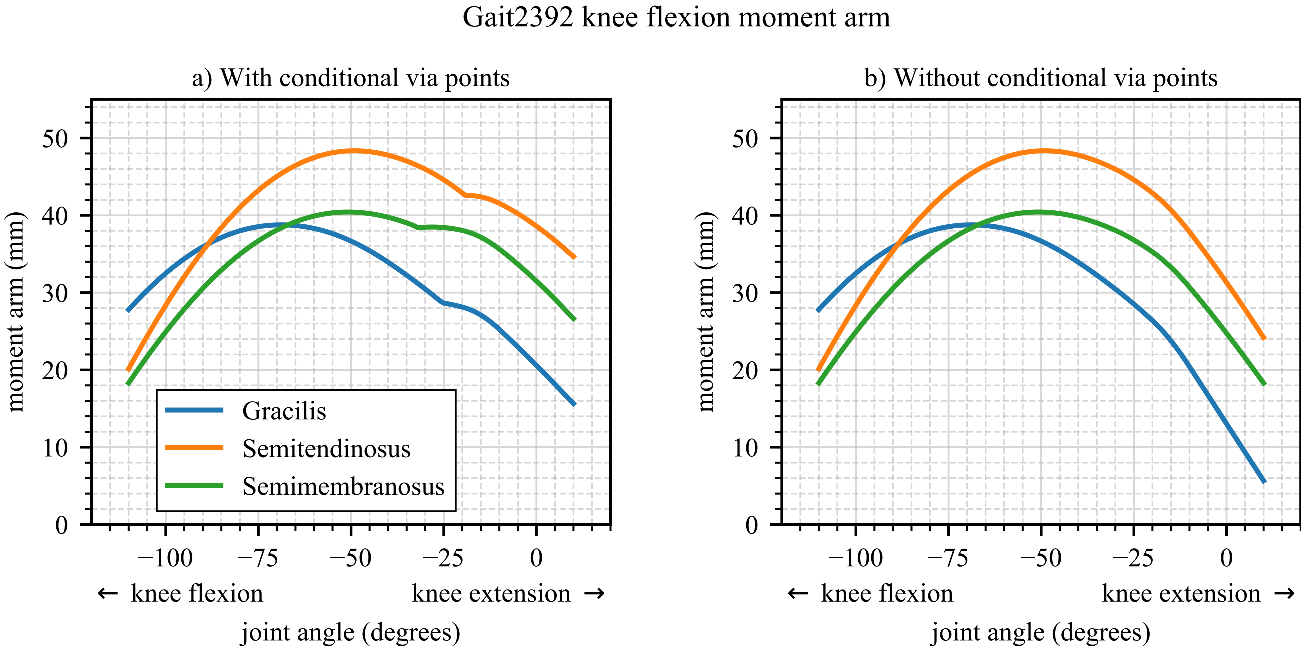

Fig. (2) a) Knee flexion muscle moment arms of the Gait2392 model, showing discontinuity due to conditional via points in muscle moment arms at 25° 32° and 19° knee flexion angle for gracilis, semitendinosus and semimembranosus respectively. b) Knee flexion muscle moment arms of the Gait2392 model where the conditional via points are removed.

sartorius knee flexion moment arms and knee flexion moment arms of the vastus muscles and rectus femoris. For sartorius knee flexion moment arms, experimental data obtained by Buford, et al. (1997) [6] was used as the target data. For the vastus muscles and rectus femoris, experimental measurements by Eijden, et al. (1987) [10] of patellar tendon moment arms was used as the target data. For these muscles, experimental data on muscle moment arms is combined with data from the Rajagopal2015 model for optimization, such that the Gait2392 model is optimized to match the experimental data as well.

The Gait2392 model is a 23 degrees of freedom musculoskeletal model, which features 92 musculotendon actuators to represent 76 muscles in the lower extremities and torso. The lower extremity joint definitions are adopted from Delp et al. (1990) [11], low back joint and anthropometry are adopted from Anderson and Pandy (1999) [12], and a planar knee model is adopted from Yamaguchi and Zajac (1989) [13]. One of the main criticisms on this model, is that the muscle parameters and the muscle path geometry is based on experimental measurements of a single subject, which was collected as part of a study by Chand, et al. (2012) [14]. Important to note is that the experimental data included with the Gait2392 model is based on a different subject than the one reported in the paper by Chand, et al. (2012) [14]. This diminishes the scientific reliability of the Gait2392 model, even though it has been widely used for both educational and research purposes [15]–[18].

The Rajagopal2015 model, created by Rajagopal, et al. (2016) [19], is a 37 degrees of freedom model with 80 musculotendon units that actuate the lower limbs and 17 torque actuators that actuate to upper body. In their paper and their supplementary material, Rajagopal, et al. (2016) show that the muscle moment arms closely match those found by experimental measurements. This is largely confirmed by the eperimental data I collected during my literature review. For most muscles, they were able to match the muscle moment arms to available experimental data well by using wrapping surfaces. However, computation time of moment arm data takes around 80x longer compared to the Gait2392 model. This makes the Rajagopal2015 model much less attractive for forward simulation studies, compared to the Gait2392 model.

The first step towards optimizing the via points of the Gait2392 model, is to remove the conditional via points, which in turn eliminates the discontinuity in the muscle parameters during joint rotations. These discontinuities can be seen when we plot the muscle moment arms as a function of joint angle

TABLE (I) Range of motion for which the muscle moment arms are optimized per degree of freedom.

Degree of freedom	Range of motion in degrees
Ankle plantar-/dorsiflexion	$[-40, 30]$
Ankle e-/inversion	$[-20, 20]$
Knee flexion/extension	$[-110, 10]$
Hip extension/flexion	$[-20, 120]$
Hip ab-/adduction	$[-40, 20]$
Hip exo-/endorotation	$[-20, 20]$

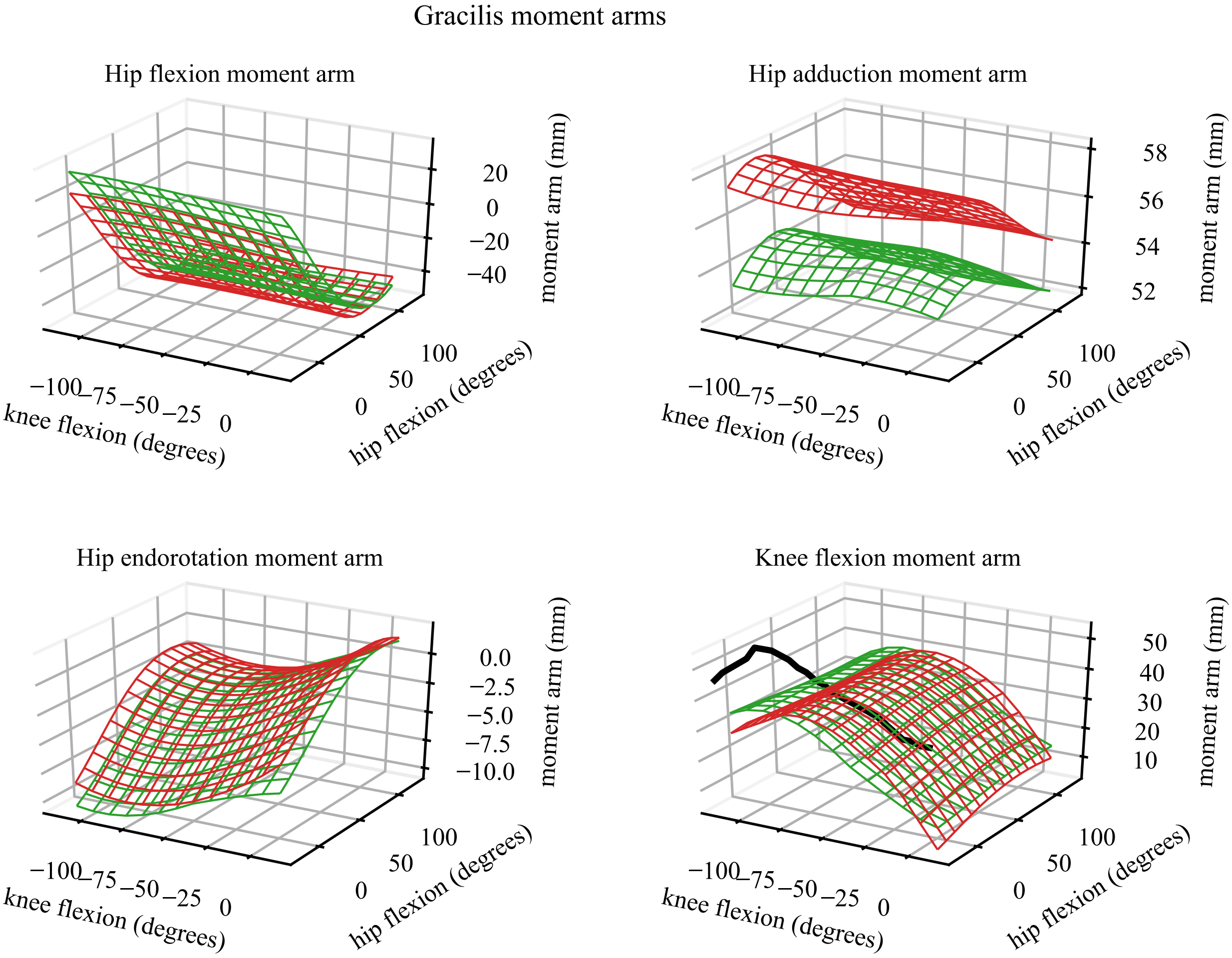

Fig. (3) Rajagopal2015, Gait2392, Experimental data from Buford, et al. (1997) [6].
Surface plots of 2D moment arms of gracilis as a function of knee and hip flexion angles for both the unoptimized Gait2392 model (without conditional via points) and the Rajagopal2015 model. 2D knee flexion moment arm data from Buford, et al. (1997) as a function of knee flexion angles is shown at 0° hip flexion, 0° hip extension and 0° knee flexion. Knee flexion angles are defined as negative angles and hip flexion angles are defined as positive values.

for muscles that are modelled with conditional via points. In Fig. 2a. this can be observed at 25° 32° and 19° knee flexion for gracilis, semitendinosus and semimembranosus respectively. Fig. 2b. shows the moment arm data of the model after removal of the conditional via points.

After removal of the conditional via points, the 3D coordinates of the via points need to be adjusted. In order to tune the via points of the Gait2392 model, an optimizer is used where the objective is to minimize the difference between the muscle moment arms of the Gait2392 model and the Rajagopal2015 model within the natural range of motion of the joints. The ranges of motion for each degree of freedom are presented in Table I. Naturally, only the muscles that are included in both models are optimized. These muscles are presented in Table II. For each muscle the 2D moment arms are computed at all combinations of joint angles that influence the length of the muscle, with intervals of 10°. This means that, for example, for gracilis four 2D moment arms are computed for 6825 joint configurations at all combinations of hip flexion, hip adduction, hip rotation and knee flexion angles, resulting in a total of 27300 data points. Surface plots of 2D moment arms of gracilis as a function of knee and hip flexion angles are shown in Fig. 3 for both the unoptimized Gait2392 model (without conditional via points) and the Rajagopal2015 model. Exeperimentally available knee flexion moment arm data, measured by Buford, et al. (1997) [6], of gracilis is also plotted. The objective of the optimization can be defined as minimizing the sum of squared errors between the computed moment arms of the Gait2392 model and the Rajagopal2015 model. For knee flexion moment arms of sartorius, we use the experimental data as the target data. The six parameters that are optimized are the x, y, z coordinates of the two via points that span the joint(s).

There are two hyperparameters of the optimization scheme.

TABLE (II) The via points of muscles that are included in both the Gait2392 and the Rajagopal2015 model are optimized. Gluteus maximus, gluteus medius, gluteus minimus and adductor magnus are divided into three components to better represent the wide origin and insertion of the muscle on the bone structures. For a clearer overview, the muscles are categorized by the degrees of freedom of the musculoskeletal model that have on effect on the length of the muscles. The 'bi-articular femur' category encompasses the muscles that span both the hip and the knee joint. The 'bi-articular tibia' category encompasses the muscles that span the knee and the ankle joint.

Category	Muscle	Gait2392	Rajagopal2015
Mono-articular hip	Gluteus maximus 1	x	x
	Gluteus maximus 2	x	x
	Gluteus maximus 3	x	x
	Gluteus medius 1	x	x
	Gluteus medius 2	x	x
	Gluteus medius 3	x	x
	Gluteus minimus 1	x	x
	Gluteus minimus 2	x	x
	Gluteus minimus 3	x	x
	Adductor longus	x	x
	Adductor brevis	x	x
	Adductor magnus 1	x	
	Adductor magnus 2	x	
	Adductor magnus 3	x	x
	Pectineus	x	
	Quadratus femoris	x	
	Gemellus	x	
	Piriformis	x	x
	Iliacus	x	x
	Psoas	x	x
Mono-articular knee	Vastus medialis	x	x
	Vastus lateralis	x	x
	Vastus intermedius	x	x
	Biceps femoris short head	x	x
Mono-articular ankle	Soleus	x	x
	Tibialis posterior	x	x
	Flexor digitorum	x	x
	Felxor hallucis	x	x
	Tibialis anterior	x	x
	Peroneus brevis	x	x
	Peroneus longus	x	x
	Peroneus tertius	x	
	Extensor digitorum	x	x
	Extensor hallucis	x	x
Bi-articular femur	Semimembranosus	x	x
	Semitendinosus	x	x
	Biceps femoris long head	x	x
	Sartorius	x	x
	Tensor fascia latae	x	x
	Gracilis	x	x
	Rectus femoris	x	x
Bi-articular tibia	Gastrocnemius medialis	x	x
	Gastrocnemius lateralis	x	x

Firstly, the user can determine how much the via points of the optimized model can deviate from the original model. It is possible that the optimization scheme finds optimal solutions for the via points that have a negative effect on other muscle parameters, such as muscle length and optimal fiber length. Furthermore, the optimal via points may disrupt the visual fidelity of the musculoskeletal model as well. Therefore, each via point is constrained to remain within 2.5 cm of the original via point. The second hyperparameter, which is only of influence when experimental data is used for the optimization, is a weight that determines how much emphasis must be put on the experimental data in relation to the model data. For example, if we look at Fig. 3d, we see that the number of data points that represents the experimental data is underrepresented in comparison to the data points computed from the Rajagopal2015 model, i.e. knee flexion moment arm is computed only as a function of knee flexion angle, while the other degrees of freedom are kept at 0°. This means that only 13 of the 27300 data points are represented by experimental data. The tuning of this weight is done manually for each of the muscles for which this is relevant.

The optimization is implemented in `Python`. The API of the `OpenSim` software package is used to compute the moment arms and to adjust the coordinates of the via points of the model. The optimization method of choice is the Nelder-Mead method [20], included in the `SciPy` optimization library, which is a non-differentiable optimization method that uses the simplex algorithm [21]. The main benefit of using a non-differentiable optimization method, is that the `Python` script can be easily modified to load and optimize other models, without needing to know how the joint kinematics are modelled.

III. Results

The results of the optimization are presented in Table III. The scores pre- and post-optimization are presented as:

$$Score = \frac{\sqrt{SSD}}{n} \quad (1)$$

where SSD is the sum of squared differences in moment arm length between the Gait2392 and the Rajagopal2015 model, and n is the number of moment arms that are computed for each muscle. In other words, it is the average difference in moment arm length. The most noticeable observation is that the muscles that contribute to practically one degree of freedom (even if they span a multi-degree-of-freedom joint), such as glutues minimus, gluteus medius and adductor brevis, are easily optimized. Optimization of muscles that exert significant moments on more than one degree of freedom tend to improve relatively worse. In the following subsections, examples of both cases will be presented in more detail.

A. Gluteus medius and gluteus minimus

The average difference of gluteus medius and gluteus minimus moment arms, beween the Rajagopal2015 and Gait2392 model, after optimization, is reduced to 0. Gluteus medius

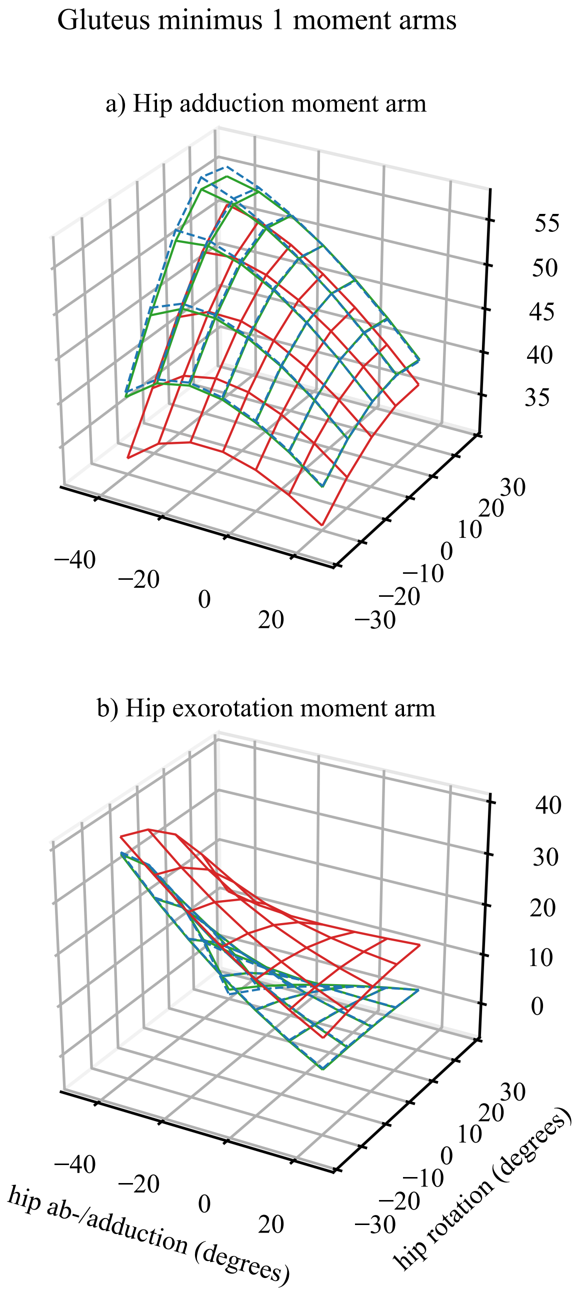

Fig. (4) —— Rajagopal2015, —— Gait2392, – – Gait2392 optimized. a) Hip abduction moment arm as a function of hip ab-/adduction and hip rotation angles. b) Hip exorotation moment arm as a function of hip ab-/adduction and hip rotation angles. Hip abduction and exorotation angles are defined as negative values. Hip adduction and endorotation angles are defined as positive angles.

TABLE (III) Average 2D muscle moment arms pre- and post-optimization. The scores are presented as $\frac{\sqrt{SSD}}{n}$, where SSD is the sum of squared differences in moment arm length between the Gait2392 and the Rajagopal2015 model, and n is the number of moment arms that are computed for each muscle.

Category	Muscle	Score pre-optimization (mm)	Score post-optimization (mm)
Mono-articular hip	Gluteus maximus 1	13.56	10.49
	Gluteus maximus 2	7.14	5.1
	Gluteus maximus 3	6.4	3.16
	Gluteus medius 1	5.39	0
	Gluteus medius 2	3.46	0
	Gluteus medius 3	3.16	0
	Gluteus minimus 1	6.78	0
	Gluteus minimus 2	5.66	0
	Gluteus minimus 3	3.47	0
	Adductor longus	6.78	3.32
	Adductor brevis	11.22	1.73
	Adductor magnus 1	-	-
	Adductor magnus 2	-	-
	Adductor magnus 3	3.32	1
	Pectineus	-	-
	Quadratus femoris	-	-
	Gemellus	-	-
	Piriformis	2.83	0
	Iliacus	10.95	5.29
	Psoas	13.38	4.47
Mono-articular knee	Vastus medialis	15.84	3
	Vastus lateralis	14.56	2.45
	Vastus intermedius	15.52	2
	Biceps femoris short head	8.25	3.16
Mono-articular ankle	Soleus	2.65	2.45
	Tibialis posterior	2.45	1
	Flexor digitorum	2.65	1
	Flexor hallucis	2	0
	Tibialis anterior	2.65	0
	Peroneus brevis	2.83	1
	Peroneus longus	2.65	0
	Peroneus tertius	-	-
	Extensor digitorum	3.16	1.73
	Extensor hallucis	3.46	2.24
Bi-articular femur	Semimembranosus	3.74	1.41
	Semitendinosus	4.58	2.65
	Biceps femoris long head	5.66	1
	Sartorius	9.22	5.9
	Tensor fascia latae	9	6
	Gracilis	5.57	3.74
	Rectus femoris	7.75	3.61
Bi-articular tibia	Gastrocnemius medialis	8.66	3.74
	Gastrocnemius lateralis	7.14	2.45

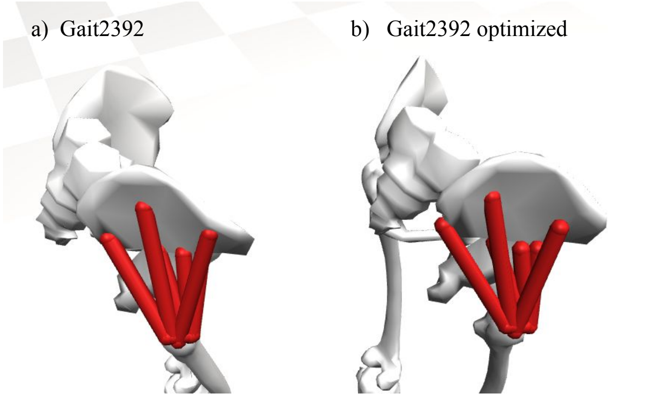

Fig. (5) a) Gluteus medius and gluteus minimus muscle paths before optimization. b) Gluteus medius and gluteus minimus muscle paths after optimization.

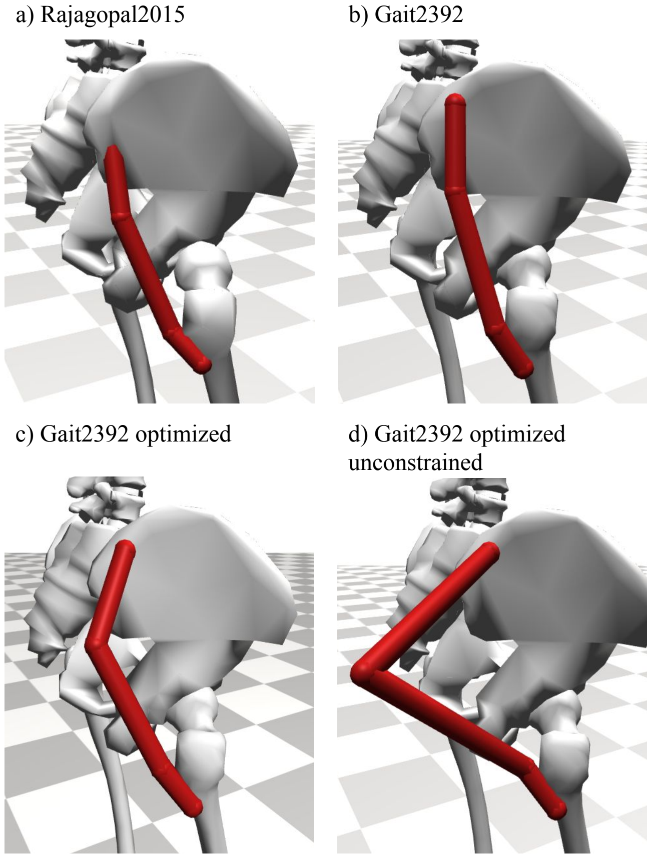

Fig. (6) Gluteus maximus 1 muscle path of Rajagopal2015 and Gait2392

and gluteus minimus mainly exert an abduction and exorotation moment around the hip. The abduction and exorotation moment arms of gluteus minimus 1 are plotted in Fig. 4 as a function of hip ab-/adduction and hip rotation angles. From these plots, it is clear that the optimization of the via points worked well for these muscles. This is most likely due to the fact that these muscles are relative short and can be represented with a straight line muscle path, as shown in Fig. 5. Besides the succes of the optimization, the visual fidelity remains good as well.

B. Gluteus maximus

The average difference of gluteus maximus 1 moment arms, beween the Rajagopal2015 and Gait2392 model, after optimization, is reduced from 13.56 mm to 10.49 mm. This a relatively small improvement, compared to other muscles. Gluteus maximus mainly exerts an extension and exorotation moment around the hip. The extension and exorotation moment arms are plotted in Fig. 4 as a function of hip extension/flexion and hip rotation angles. From Fig. 4a, it is clear that during hip flexion angles the differences in hip extension moment arms become increasingly larger. The Rajagopal2015 model is able to maintain a more constant moment arm because of the use of wrapping surfaces. For testing purposes, the optimization is also done whithout the positional constraints on the via points, i.e. they are not constrained to remain within 2.5 cm of the original via point. This reduced the difference between the models to 7.4 mm. However, removal of the postional constraints changes the trend of moment arms as a function of hip joint angles, lengthens the muscle fiber lenght significantly and reduces the visual fidelity of the model as well, as seen in Fig. 4d. It seems that the effect of wrapping surfaces can not be captured well with via points.

C. Vastus muscles

The average difference of vastus medialis, vastus lateralis and vastus intermedius is reduced by 81%, 83% and 87% respectively. However, the visual fidelity of vastus intermedius and vastus medialis is reduced after optimization, which is seen in Fig. 8b. Fortunately, this can be easily corrected by adjusting the surrounding via points, since these via points do not have any effect on the muscle moment arm. However, the manual adjustments seen in Fig. 8c alter the length of the muscle, which has to be accounted for by adjusting the optimal fiber length and the tendon slack length.

D. Gracilis

Experimentally measured sartorius knee flexion moment arms are longer than those included in the Rajagopal2015 model. Therefore, the knee flexion moment arm as a function of knee flexion angle (all other degrees of freedom are kept at 0°) is optimized to fit experimental data from Buford, et al. (1997) [6], while moment arms for all other data points are taken from the Rajagopal2015 model. We see that indeed the optimization process optimizes the via points such that the muscle moment arms matches the experimentally obtained knee flexion moment arms more than data from Rajagopal2015, while simultaneously improving hip flexion, hip adduction and hip endorotation moment arms. Because only 13 of the 27300 data points are represented by experimental data, the weights were set such that the differences between the Gait2392 moment arms and the experimental data contribute 80% to the sum of squared differences.

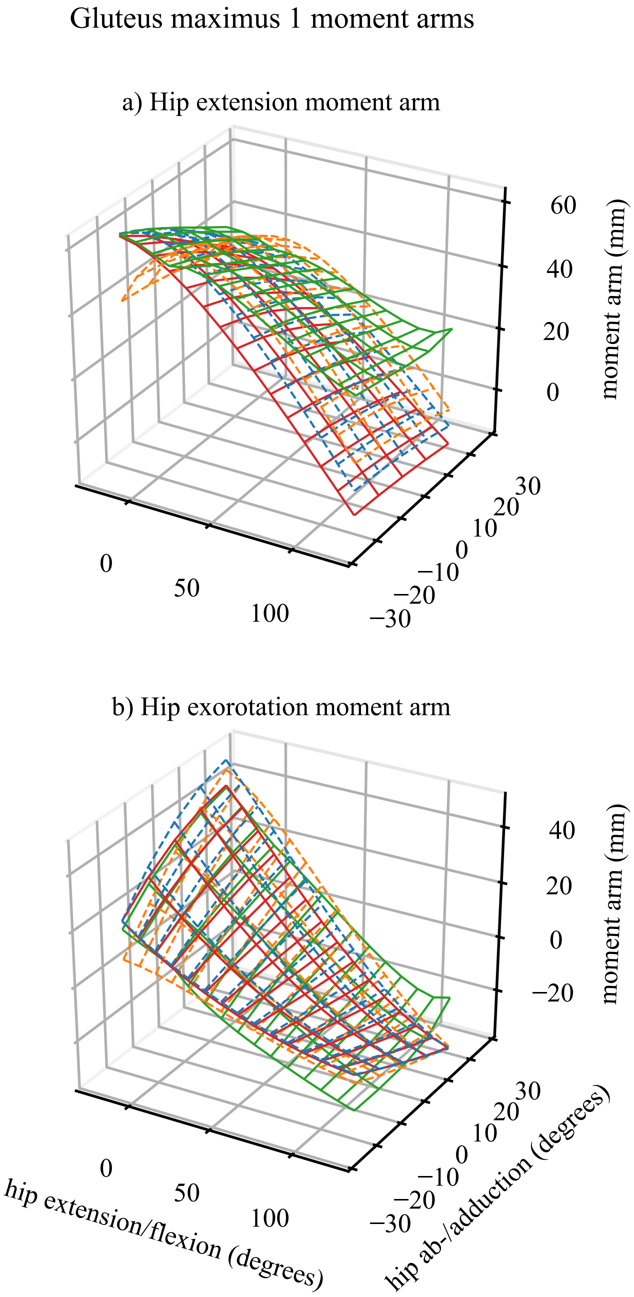

Fig. (7) Rajagopal2015, Gait2392, Gait2392 optimized, Gait2392 optimized with unconstrained via points. a) Hip flexion moment arm as a function of hip extension/flexion and hip ab-/adduction angles. b) Hip exorotation moment arm as a function of hip extension/flexion and hip ab-/adduction angles. Hip flexion and adduction angles are defined as positive values. Hip extension and abduction angles are defined as negative angles.

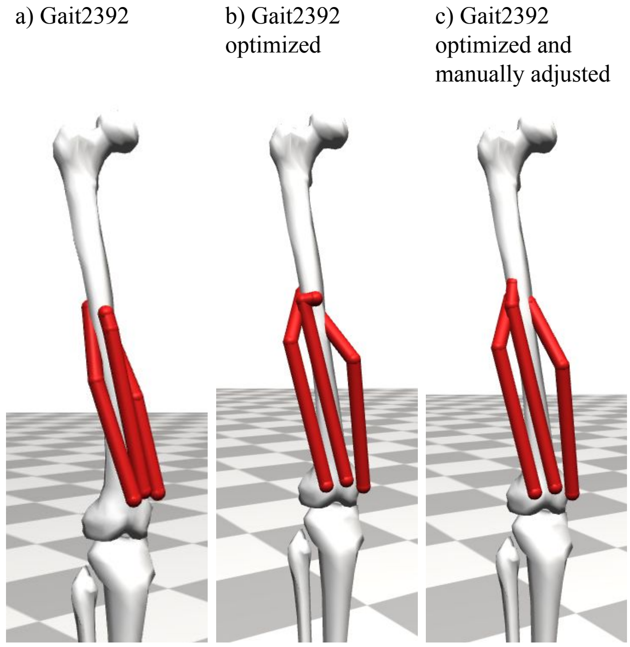

Fig. (8) Muscle paths of vastus laterlis, vastus intermedius and vastus medialis.

IV. Discussion

The results of this research show that the optimization of the via points reduces the difference in muscle moment arms between the Gait2392 and the Rajagopal2015 model. Furthermore, it is shown that experimental moment arm data, which is often measured in a single plane, can also be injected into the optimization. Others can use the `Python` script and the available data set on moment arms, which was created during my literature study, to create computationally efficient musculoskeletal models for their own purposes. Moment arm calculations for the optimized Gait2392 model are around 80x faster than the Rajagopal2015 model, which makes a significant difference when using the optimized Gait2392 model in forward simulation studies.

However, there are also some caveats with the validity of the optimized model. First of all, not all muscles are improved in terms of muscle moment arm length, and moreover, in terms of the trend of the moment arm as a function of joint angle. An example was given for gluteus maximus 1, where the wrapping surface of the Rajagopal2015 model ensures that the moment arm remains relatively constant, which could not be captured with via points. Gluteus maximus is a large muscle, with a large pennation angle, making it the main contributor to hip extension moments [22]. If this muscle is not represented well within a model, the biological fidelity is diminished significantly. However, here we optimized the muscle moment arm of gluteus maximus to match the data obtained from the Rajagopal2015 model. To date, there is no experimental data available on gluteus maximus moment arms as a function of

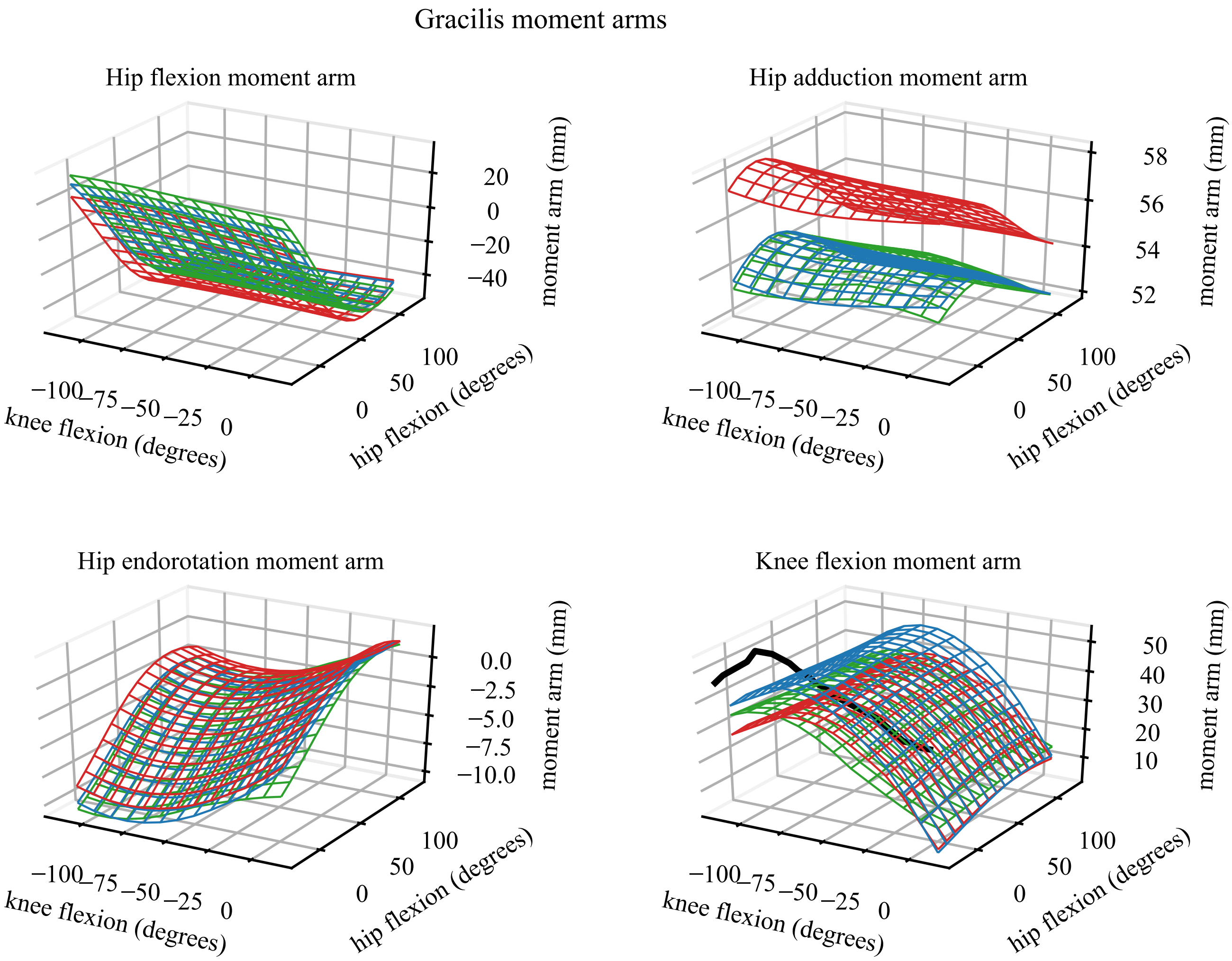

Fig. (9) Rajagopal2015, Gait2392, Experimental data from Buford, et al. (1997) [6], Gait2392 optimized. a) Hip flexion moment arm as a function of hip extension/flexion and hip ab-/adduction angles. b) Hip exorotation moment arm as a function of hip extension/flexion and hip ab-/adduction angles. Hip flexion and adduction angles are defined as positive values. Hip extension and abduction angles are defined as negative angles.

hip joint angles. Therefore, the accuracy of gluteus maximus moment arms is undefined for any musculoskeletal model made so far. This ties in with the next limitation: there is not enough experimental data on muscle moment arms to accurately define muscle paths. Existing experimental methods give inconsistent results in terms of moment arm data. It is still unknown how much of this inconsistency can be attributed to the different measuring methods, to the errors induced by the person(s) that executed the experiments, or to the physiological differences of the subjects that participated in these experiments. In order to create good musculoskeletal models that represent the biological systems well, there is a strong need to revisit the way we measure muscle moment arms.

Another limitation of the proposed method is that after optimization other muscle parameters, such as tendon slack length and optimal fiber length, have to be retuned. This is especially true for muscles that have to be manually tuned to improve the visual fidelity of the model, as is the case with the vastus muscles. However, in future work, this can be added to the optimization scheme.

There are also some benefits to this method, and even to this model. For example, when using forward simulations to optimize a neuromuscular controller, one could first pre-train the neuromuscular controller with the computationally efficient model to obtain a set of controller parameters that can be further fine-tuned using the more complex model. This can still greatly increase the optimization time, which was the purpose of this research to begin with. Furthermore, it would be interesting to continue this research and add trunk and upper extremity muscles using this same method, where the coordinates of the via points are optimized to match existing, more complex, models and experimental data. The more complete the musculoskeletal model is, the more beneficial it will be to have a computationally efficient model.

ACKNOWLEDGMENTS

Thomas Geijtenbeek (Supervisor) & Frans van der Helm (Supervisor).

REFERENCES

[1] A. V. Hill, "The heat of shortening and the dynamic constants of muscle," *Proceedings of the Royal Society of London. Series B-Biological Sciences*, vol. 126, no. 843, pp. 136–195, 1938.

[2] S. S. Blemker and S. L. Delp, "Three-dimensional representation of complex muscle architectures and geometries," *Annals of biomedical engineering*, vol. 33, no. 5, pp. 661–673, 2005.

[3] V. T. Inman, "Functional aspects of the abductor muscles of the hip," *JBJS*, vol. 29, no. 3, pp. 607–619, 1947.

[4] T. Geijtenbeek, "Animating virtual characters using physics-based simulation," Ph.D. dissertation, Utrecht University, 2013.

[5] A. S. Arnold, S. Salinas, D. J. Hakawa, and S. L. Delp, "Accuracy of muscle moment arms estimated from mri-based musculoskeletal models of the lower extremity," *Computer Aided Surgery*, vol. 5, no. 2, pp. 108–119, 2000.

[6] W. L. Buford, F. M. Ivey, J. D. Malone, R. M. Patterson, G. Pearce, D. K. Nguyen, and A. A. Stewart, "Muscle balance at the knee-moment arms for the normal knee and the acl-minus knee," *IEEE Transactions on Rehabilitation Engineering*, vol. 5, no. 4, pp. 367–379, 1997.

[7] W. Herzog and L. Read, "Lines of action and moment arms of the major force-carrying structures crossing the human knee joint." *Journal of anatomy*, vol. 182, no. Pt 2, p. 213, 1993.

[8] C. Spoor and J. Van Leeuwen, "Knee muscle moment arms from mri and from tendon travel," *Journal of biomechanics*, vol. 25, no. 2, pp. 201–206, 1992.

[9] P. Wretenberg, G. Nemeth, M. Lamontagne, and B. Lundin, "Passive knee muscle moment arms measured in vivo with mri," *Clinical Biomechanics*, vol. 11, no. 8, pp. 439–446, 1996.

[10] T. Van Eijden, W. Weijs, E. Kouwenhoven, and J. Verburg, "Forces acting on the patella during maximal voluntary contraction of the quadriceps femoris muscle at different knee flexion/extension angles," *Cells Tissues Organs*, vol. 129, no. 4, pp. 310–314, 1987.

[11] S. L. Delp, J. P. Loan, M. G. Hoy, F. E. Zajac, E. L. Topp, and J. M. Rosen, "An interactive graphics-based model of the lower extremity to study orthopaedic surgical procedures," *IEEE Transactions on Biomedical engineering*, vol. 37, no. 8, pp. 757–767, 1990.

[12] F. C. Anderson and M. G. Pandy, "A dynamic optimization solution for vertical jumping in three dimensions," *Computer methods in biomechanics and biomedical engineering*, vol. 2, no. 3, pp. 201–231, 1999.

[13] G. T. Yamaguchi and F. E. Zajac, "A planar model of the knee joint to characterize the knee extensor mechanism," *Journal of biomechanics*, vol. 22, no. 1, pp. 1–10, 1989.

[14] C. T. John, F. C. Anderson, J. S. Higginson, and S. L. Delp, "Stabilisation of walking by intrinsic muscle properties revealed in a three-dimensional muscle-driven simulation," *Computer methods in biomechanics and biomedical engineering*, vol. 16, no. 4, pp. 451–462, 2013.

[15] C. D. Walck, Y. Lim, T. J. Farnese, V. Huayamave, D. C. Osbahr, and T. N. Furman, "The effect of non-linear spring-loaded knee orthosis on lower extremity biomechanics," in *International Symposium on Computer Methods in Biomechanics and Biomedical Engineering*. Springer, 2019, pp. 371–383.

[16] M. Żuk and C. Pezowicz, "The influence of uncertainty in body segment mass on calculated joint moments and muscle forces," in *Conference of Information Technologies in Biomedicine*. Springer, 2016, pp. 349–359.

[17] Y. Kim, Y. Jung, W. Choi, K. Lee, and S. Koo, "Similarities and differences between musculoskeletal simulations of opensim and anybody modeling system," *Journal of Mechanical Science and Technology*, vol. 32, no. 12, pp. 6037–6044, 2018.

[18] J. F. Oeding, "Quantifying coordination of human gait: fall risk and effects of aging," Ph.D. dissertation, Massachusetts Institute of Technology, 2019.

[19] A. Rajagopal, C. L. Dembia, M. S. DeMers, D. D. Delp, J. L. Hicks, and S. L. Delp, "Full-body musculoskeletal model for muscle-driven simulation of human gait," *IEEE transactions on biomedical engineering*, vol. 63, no. 10, pp. 2068–2079, 2016.

[20] J. A. Nelder and R. Mead, "A simplex method for function minimization," *The computer journal*, vol. 7, no. 4, pp. 308–313, 1965.

[21] G. B. Dantzig, "Origins of the simplex method," in *A history of scientific computing*, 1990, pp. 141–151.

[22] R. Putz and R. Pabst, *Sobotta-Atlas of Human Anatomy: Head, Neck, Upper Limb, Thorax, Abdomen, Pelvis, Lower Limb; Two-volume set.*, 2006.